論 文

# [1168] DEVELOPMENT LENGTH OF BRAIDED ARAMID FIBER TENDONS IN PRETENSIONED BEAMS

By Toru. UTSUNOMIYA*, Antonio. NANNI**, Hiroyuki. YONEKURA*
and Masaharu. TANIGAKI*

## 1. INTRODUCTION

Development length of prestressing tendons is a fundamental design parameter in pretensioned concrete members. The development length ($L_d$) is defined as the tendon embedment length necessary to develop the nominal flexural capacity of a member and can be subdivided into transfer length ($L_t$) and flexural bond length ($L_f$) as shown in Fig. 1. This figure shows the ideal stress distribution along the tendon of a simply-supported beam subjected to a concentrated load (disregarding self-weight) when flexural and tendon anchorage capacity are reached simultaneously. The stress in the tendon due to the moment distribution is superimposed to the stress due to prestressing. The beam can be divided into cracked region ($M>M_{cr}$) and uncracked region ($M<M_{cr}$). The discontinuity in tendon stress at the threshold between the two regions and the different stress gradients result from the substantial difference between cracked and uncracked section moduli($Z_{cr}$ and $Z_{uc}$) which are for simplicity assumed to be constant. In this figure, tendon stress concentration at the location of cracks is not considered. Tendon anchorage failure conceivably occurs when the bond strength is overcome or splitting crack occurs in the concrete region included between the end of the transfer length and the cross section with $M=M_{cr}$.

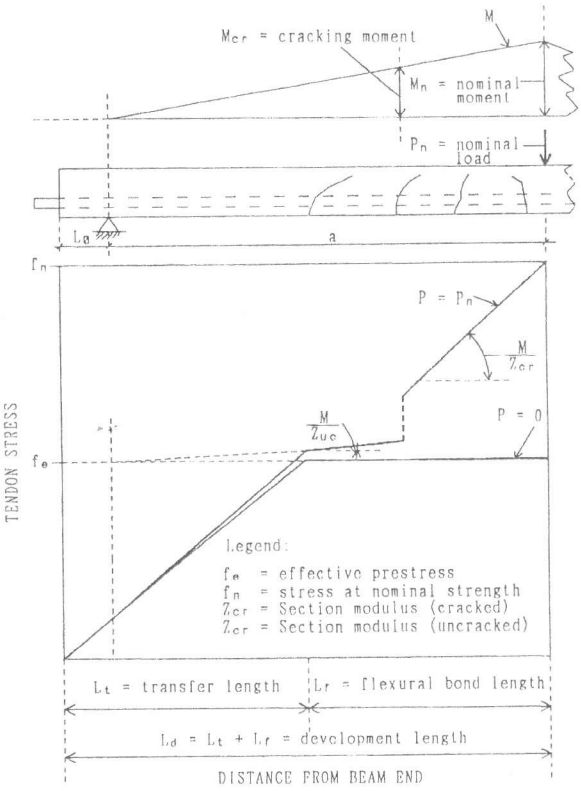


**Fig. 1 : Ideal Stress Distribution**

The objective of this experimental study was to determine the value of $L_d$ for braided epoxy-impregnated aramid fiber (AF) tendons of the flexible type. The characteristics of materials and specimens used in this project were reported in a companion paper published in these proceedings [1]. Ref. 1 presents the experimental results and the discussion relative to the determination of transfer length.

* Technical Research Institute, Mitsui Construction Co.
** Dept. of Architectural Engineering, The Pennsylvania State University

## 2. TEST PROGRAM

Specimen cross-sections with tendon and reinforcement details are shown in Fig. 2-a. The 4-m long specimens were tested in accordance with one of the two set-ups shown in Fig. 2-b and 2-c. In the standard configuration (Fig. 2-b), the applied load was positioned at a predetermined distance from one of the beam-ends (L). The load-point was at the center of the simply-supported span ($L_s$) with first support (A) always at 15 cm from the beam end. At a distance $L_s$ from the second support (B), a constant force ($F_j$) was provided by a mechanical jack so that the moment at B was maintained equal to 0 throughout the test. This test set-up was chosen because of its stability even in the event of brittle failure. The picture in Fig. 3 shows a specimen under testing in the laboratory. Using the standard configuration, it was possible to limit the damage (cracking) to one of the beam sides, so that a second test could be performed on the opposite side in accordance to standard or alternate configuration (Fig. 2c). Test instrumentation consisted of load cells, strain gages mounted on concrete and tendons, and linear variable differential transformers (LVDT's) for the measurement of beam deflection and tendon slippage. A detail of the instrumentation at the beam end is shown in Fig. 4. Samples showed either flexural failure or tendon anchorage failure (in some cases both failures occurred simultaneously). Flexural failure was characterized by crushing of the concrete in the compressive zone or by combination of crushing and shear failure (when shear reinforcement was not present). Beams were designed so that AF tendon breaking would not occur prior to concrete crushing. Tendon anchorage failure was in the form of tendon slippage with or without the formation of visible concrete split-cracking parallel to the tendon axis. Depending on the type of failure recorded at the first beam-end, the experimental value of L was varied:

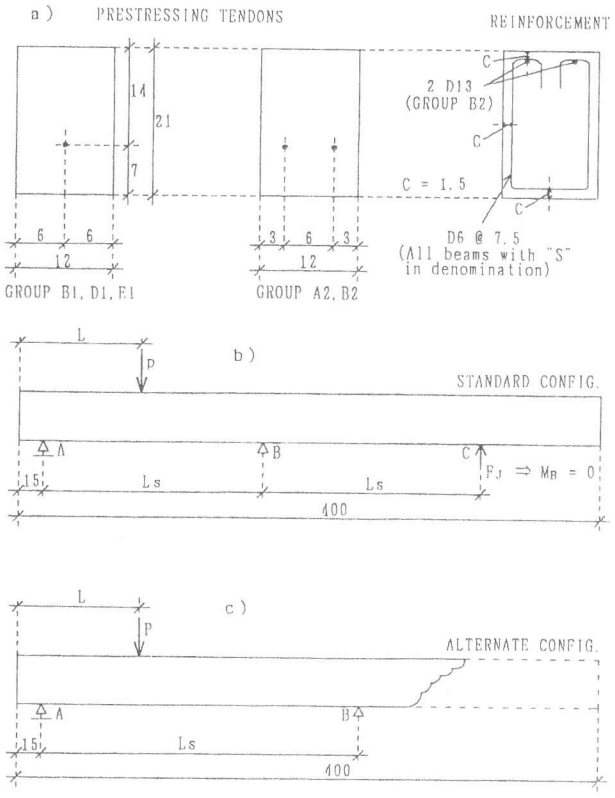


Fig. 2 : Beam Cross-section Types and Test Set-up Configurations (Dimensions in cm)

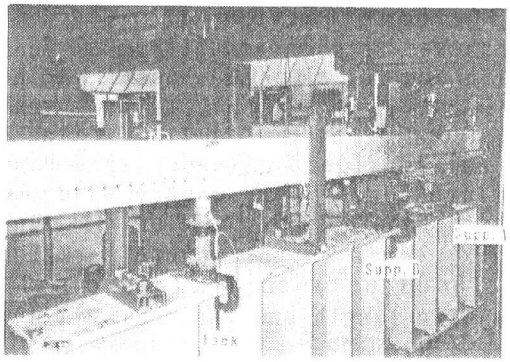

Fig. 3 : Test According to Standard Set-up Configuration

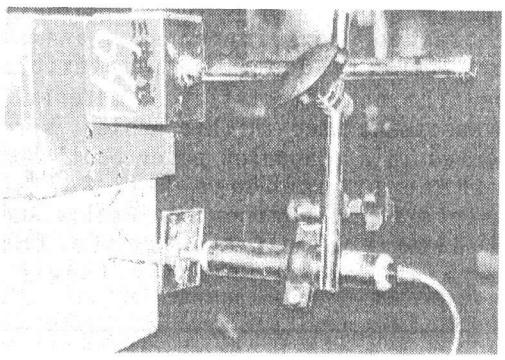

Fig. 4 : Detail of Beam-end Instrumentation

decreased in case of flexural failure or otherwise increased. This procedure of successive approximation was repeated for all beams in each group.

## 3. RESULTS AND DISCUSSION

The experimental results reported in Table 1 are a comprehensive summary of all development length tests. The first column in the table shows beam denomination and side subjected to test (F=fixed-end, J=jack-end). The letter "S" in the specimen denomination indicates the presence of shear reinforcement (see Fig. 1). The second column shows the tendon type and number. In the third column, the values of transfer length as determined in Ref. 1 for the same specimens are given. $L_t$ values were influenced by tendon type and size as well as concrete strength or time of release. Finally, the last three columns in the table show cracking moment ($M_{cr}$), ultimate moment ($M_u$) and beam failure type. For beams where anchorage failure occurred (symbols B and BS in the table), once the tendon-end moved approximately 0.002 mm, progressive slip occurred even if the applied load was decreased. For the four beams shown to have reached a simultaneous anchorage and flexural failure, tendon slippage occurred only after concrete cracks on the top surface of the beam had formed. It is not the objective of this paper to present a discussion on flexural capacity of prestressed concrete beams. However, the following remarks can be made:

- Experimental data for both cracking and ultimate moment capacity showed good agreement with expected values.
- Beams reinforced with stirrups showed an ultimate moment capacity slightly higher than that of beams with no shear reinforcement. The shear-span to reinforcement depth (a/d) ratio for beams with stirrups was between 5 and 10.7. For beams with no stirrups the a/d ratio ranged between 5.7 and 13.2.
- As expected, beams which failed because of tendon anchorage slippage showed lower ultimate moment.

An example of data collected during a test is shown in Fig.s 5 and 6 for the case of beam B1-2 (F) in the standard set-up configuration (Fig. 2: L= 100 cm, $L_s$=170 cm, Fj=75 kg (0.73 kN)). Fig. 5 shows the experimental load-deflection curve. The deflection under the load point is the net value adjusted for support settlement. Beam failure resulted from concrete crushing (ultimate concrete strain at 1-cm depth equal to 2754x10-6) followed by bond slip. Bond slip started at a post-peak load of 2.64 t (25.9 kN) and continued even after complete unloading of the beam. The total bond slip during the unloading stage was 0.045 mm.

**Table 1 : Experimental Data**

| Beam Denom. (Side) | Tendon Type-Number | Transfer Length Lt (cm) | Load Position L (cm) | Supported Span Ls (cm) | Cracking Moment (kgcm) | Ultimate Moment (kgcm) | Failure Type* |
|---|---|---|---|---|---|---|---|
| A2-1 (J) | K64-2 | 20 | 95 | 160 | 59654 | 125492 | BS |
| A2-2 (J) | K64-2 | 30 | 100 | 170 | 63601 | 124801 | BS |
| A2-2 (F) | K64-2 | 30 | 110 | 190 | 52523 | 121873 | FV |
| A2-S (J) | K64-2 | 20 | 95 | 160 | 59304 | 148904 | F |
| A2-S (F) | K64-2 | 20 | 85 | 140 | 59179 | 166979 | BS + F |
| B1-1 (F) | K128-1 | 50 | 105 | 180 | 56624 | 137024 | FV |
| B1-1 (J) | K128-1 | 50 | 95 | 160 | 51844 | 126644 | BS |
| B1-2 (F) | K128-1 | 40 | 100 | 170 | 62306 | 127586 | BS + FV |
| B1-2 (J) | K128-1 | 40 | 100 | 170 | 62306 | 106506 | FV |
| B1-S (J) | K128-1 | 30 | 110 | 190 | 55967 | 148434 | F |
| B1-S (F) | K128-1 | 30 | 95 | 160 | 59044 | 146644 | F |
| B1-SF (J) | K128-1 | 30 | 85 | 140 | 59844 | 148394 | B |
| B1-SF (F) | K128-1 | 30 | 90 | 150 | 54343 | 160618 | B + F |
| B2-S-1(J) | K128-2 | 40 | 105 | 180 | 89914 | 238414 | F |
| B2-S-1(F) | K128-2 | 40 | 95 | 160 | 94464 | 252864 | BS + F |
| E1-1 | SWPR7A | 145 | 200 | 370 | 135221 | 190721 | B |
| E1-2 | SWPR7A | 125 | 200 | 370 | 131521 | 214771 | FV |
| E1-S | SWPR7A | 115 | 165 | 300 | 122551 | 209551 | B |

*Legend : B=tendon slip F=concrete crushing
BS=tendon slip/split cracking FV=crushing/shear failure

Fig. 6 shows the flexural strain distribution along the tendon at five levels of the applied load from 1.42 to 2.96 t (13.9 to 29.0 kN). The strain was measured with 11 strain gages attached at intervals of 20 cm. The first strain gage was positioned 15 cm outside the concrete and cut-off after tendon release. When a gage failed during the test, the data-points for that gage were discontinued . The first load level corresponds to the reading just before first-crack. The last load level corresponds to the ultimate capacity. Above the strain diagrams, the beam crack patterns for the corresponding load levels are also shown. A very small strain increment in the tendon is observed before first-crack. Beyond first-crack, the location of cracks strongly influences the strain distribution in the tendon. Measured strain values in the cracked central region are below the analytically computed values. This is because of stress transfer to sound concrete between two flexural cracks. From Fig. 6, it is apparent that strain in the tendon decreases very rapidly outside the cracked central region.

Since beam B1-2 (F) experienced simultaneous flexural and anchorage failure, the diagram presented in Fig. 2 can be redrawn using measured strain values. This is done in Fig. 7 where the strain distribution in the tendon up to the load point (100 cm) is shown at six different ages. The first curve (which is practically a constant line at 4500 microstrain) represents the strain in the tendon 12 hours after casting. The following curve represents the strain distribution at age 14-day just before tendon release. The strain in the first 20-cm of the beam increases as the tendon restrains concrete shrinkage, whereas in the central portion of the beam the strain stabilizes at 4000 microstrain. The third curve shows the strain distribution immediately after tendon release: beyond transfer length the strain value in the mid-span region drops another 70 microstrain due to

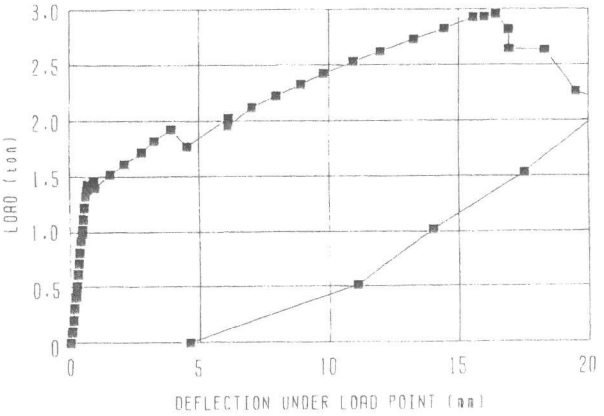


Fig. 5 : Load Deflection Curve for Beam B1-2(F)

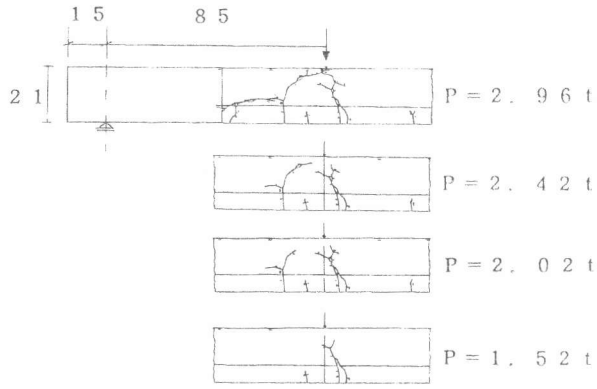


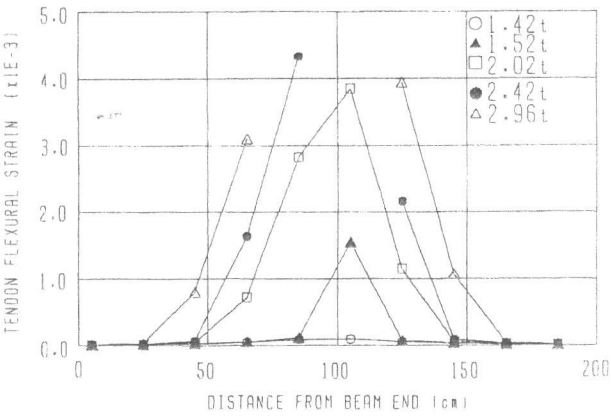


Fig. 6 : Crack Distribution and Tendon Strain for Beam B1-2(F)

Table 2 : Summary of Transfer, Flexural Bond, and Development Length

| Tendon Type & No. | Nominal Diam. (mm) | Pre-stress Force (%$P_u$) | Concrete Strength at Release (kg/cm$^2$) | Min. Tendon Cover (mm) | Transfer Length (No. of diam.) | Flexural Bond Length (No. of diam.) | Develop. Length (No. of diam.) |
|---|---|---|---|---|---|---|---|
| K64-2 | 8 | 25 | 297-325 | 26 | 25-38 | 94-100 | 125-138 |
| K64-2* | 8 | 25 | 353 | 26 | 25 | 82 | 107 |
| K128-1 | 12 | 25 | 297-325 | 54 | 34-42 | 38-50 | 80-84 |
| K128-1* | 12 | 25 | 353 | 54 | 25 | 50 | 75 |
| K128-2* | 12 | 25 | 297 | 24 | 34 | 46 | 80 |
| SWPR7A | 12.4 | 75 | 297-325 | 54 | 101-117 | 45-61 | 162 |
| SWPR7A* | 12.4 | 75 | 353 | 54 | 93 | >40 | >133 |

Note: *Stirrups D6 at 75 mm on centers

elastic shortening. The forth curve represents the strain distribution at age 72-day just before testing. The total strain loss (excluding relaxation) is approximately 900 microstrain (20% loss). The fifth curve shows the strain distribution during the flexural test when the applied load was 2.02 t (19.8 kN). The strain recorded by the gage at 85-cm is much smaller than the value derived analytically for a cracked section (>9000 microstrain). The final curve shows the strain distribution at ultimate load when tendon slippage starts to occur. As for the previous curve, the gage at 65-cm shows a value below the analytical correspondent (>9000 microstrain). The most important observation at this point is that slippage for this tendon occurs when, in the uncracked concrete zone, the strain gradient in the tendon due to flexural stress becomes equal to that measured over the transfer length.

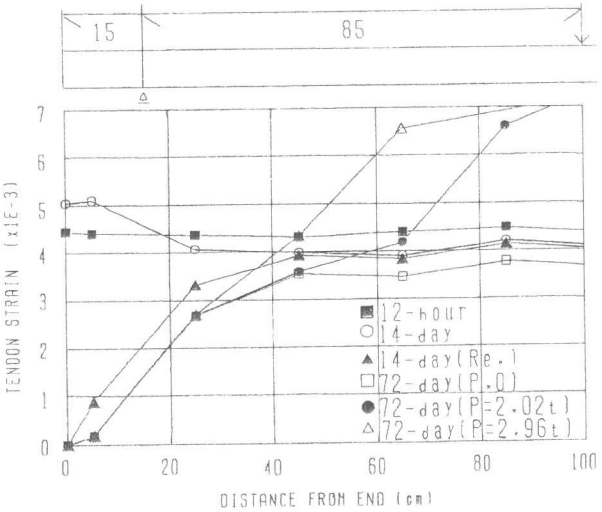


Fig. 7 : Tendon Strain Distribution for Beam B1-2 (F) at Ages Between 12-hour and 72-day

On the basis of the experimental results, development length (expressed in number of tendon diameters) for two types of aramid fiber tendons and a seven-wire steel strand were derived as presented in Table 2. This table shows seven different combinations (rows) since the case of single or double tendon and beam with or without shear reinforcement were considered separately. Even though more tests should be conducted, it is possible to make the following observations:

- The development length of tendon K128 decreases if stirrups are present as they prevent the propagation of concrete split-cracks. When two tendons are used (and the minimum cover reduced to half), $L_d$ does not change significantly if stirrups are present. Flexural bond length is approximately 1 to 2 times the value of transfer length and its magnitude is greatly affected by the position of the flexural cracks.

- $L_d$ of small diameter K64 tendons is 35 to 55% larger than that of K128 tendons. $L_f$ is 2.5 to 3.5 times the corresponding Lt. It is therefore apparent that this tendon size has a smaller anchorage efficiency in tension. This could be the consequence of the relatively small deformation of the K64 tendon surface due to the braiding of strands made with half the number of yarns. This performance was not observed in the case of transfer length (compression anchorage) where the wedging effect due to the Poisson's ratio may be more important than surface deformation.
- Seven-wire steel strands have a relatively large value of Ld. Data obtained in this study favorably compare with previous research [2] where transfer length and development length of equal diameter strands were measured at 102 and 238 diameters, respectively. In light of these experimental results, the Japanese building codes [3,4] should probably consider (or reconsider) establishing conservative values of Lt and Ld for the design of prestressed concrete members using conventional steel strand tendons.

## 4. CONCLUSIONS

The experimental determination of development length for pretensioned prestressed concrete beams shows a good performance for epoxy-impregnated aramid fiber tendons of the flexible type. The following conclusions can be drawn:

1. The shortest $L_d$ values are obtained K128 tendon. For K128-type rods, normal strain distribution along the tendon seems to indicate that anchorage failure occurs when the strain gradient in the flexural bond length region approaches the strain gradient measured over the transfer length region.
2. The development length of K64 tendon is longer than that of K128. In particular, the flexural bond length of K64 tendon is long. This may be due to smaller deformations on the K64 tendon surface.
3. The number of AF tendons per member cross-section does not significantly affect development length.
4. As expected from results on transfer length published elsewhere [1], the development length of conventional steel wire strand is longer than that of aramid fiber tendon of the same diameter. Better anchorage efficiency of AF vs. steel may result from effective AF tendon surface deformation and high Poisson's ratio.

## ACKNOWLEDGEMENTS

The second author gratefully acknowledges the support of the National Science Foundation under Grant No. MSM-8918592 for his long-term research visit to Mitsui Construction Co., Japan.

## REFERENCES

1) Nanni, A. et al., "Transfer Length of Braided Aramid Fiber Tendons," Proceedings of the Japan Concrete Institute, Vol. 13, No. 2, 1991.
2) Cousins, T.E. et al., "Development Length of Epoxy-Coated Prestressing Strand," ACI Materials J., V. 87, No. 4, Jul.-Aug. 1990, pp. 309-318.
3) Architectural Institute of Japan, "Standard for Structural Design and Construction of Prestressed Concrete Structures," 1987, pp. 222-227.
4) Japan Society of Civil Engineers, "Standard Specification for Design and Construction of Concrete Structures," Part 1-Design, 1986, pp. 159-163.